Particle Emissions, Volatility, and Toxicity from an Ethanol Fumigated Compression Ignition Engine

NICHOLAS C. SURAWSKI, †, ‡ BRANKA MILJEVIC, † BOYD A. ROBERTS, † ROBIN L. MODINI, † RONG SITU, ‡ RICHARD J. BROWN, ‡ STEVEN E. BOTTLE, § AND ZORAN D. RISTOVSKI*, †

International Laboratory for Air Quality and Health, Queensland University of Technology, GPO Box 2434 ,Brisbane QLD 4001, Australia, School of Engineering Systems ,Queensland University of Technology, GPO Box 2434,Brisbane QLD 4001, Australia, and ARC Centre of Excellence for Free Radical Chemistry and Biotechnology, Queensland University of Technology, GPO Box

Abstract:

Particle emissions, volatility, and the concentration of reactive oxygen species (ROS) were investigated for a pre-Euro I compression ignition engine to study the potential health impacts of employing ethanol fumigation technology. Engine testing was performed in two separate experimental campaigns with most testing performed at intermediate speed with four different load settings and various ethanol substitutions. A scanning mobility particle sizer (SMPS) was used to determine particle size distributions, a volatilization tandem differential mobility analyzer (V-TDMA)wasused to explore particle volatility, and a new profluorescent nitroxide probe, BPEAnit, was used to investigate the potential toxicity of particles. The greatest particulate mass reduction was achieved with ethanol fumigation at full load, which contributed to the formation of a nucleation mode. Ethanol fumigation increased the volatility of particles by coating the particles with organic material or by making extra organic material available as an external mixture. In addition, the particle-related ROS concentrations increased with ethanol fumigation and were associated with the formation of a nucleation mode. The smaller particles, the increased volatility, and the increase in potential particle toxicity with ethanol fumigation may provide a substantial barrier for the uptake of fumigation technology using ethanol as a supplementary fuel.

1. Introduction:

The transportation sector is in urgent need of alternative fuels because of the peak oil scenario and the growing global demand for transport and the accompanying increase in greenhouse gas emissions (*1*). Biofuels are being pursued as a replacement for diesel in the transportation sector to facilitate global warming mitigation, to reduce exhaust missions, and also for energy security reasons (*2, 3*). Ethanol is one example of an oxygenated biofuel that is being explored as a potential replacement for diesel in heavy-duty compression ignition (CI) engines (*4, 5*).

Several ethanol substitution technologies are available for use in CI engines and include the use of ethanol blends, ethanol emulsions, a spark ignition approach, ignitionassisting additives, dual injection of diesel and ethanol, and ethanol fumigation (*6, 7*). The ethanol fumigation approach involves delivering ethanol vapor to the intake manifold of an engine (*7*) and complements the existing literature on methanol fumigation (*8, 9*).Upto 50% of the total fuel energy at full load can be provided through ethanol fumigation, which lies between the energy substitutions achievable by blends (∼25%) and dual injection (∼90%) (*6*). The European Union is committed to a 10% substitution (by energy) of transportation fuel by renewable sources by 2020 (*10*), so it is possible that fumigation technology may play a vital role in achieving this outcome.

A well-documented advantage of ethanol usage in CI engines is the significant reduction in particulate mass emissions especially at full-load operation (*6, 11*). Despite this, a reduction in the mass of particulates emitted by an engine may not be the most appropriate metric for assessing the potential health effects of diesel particulate matter. For example, a study by Peters et al. (*12*) showed that respiratory health effects in asthma sufferers were related more strongly to the number of ambient ultrafine particles rather than to the mass (measured asPM10) of ambient particulates. In light of these observations, the measurement of particle number distributions from ethanol combustion in CI engines is an emerging area of research interest with several recent papers having been published on this topic (*11, 13–15*). This study represents the first attempt to address the issue of particle number distributions from CI engines that employ ethanol fumigation.

Previous research has addressed the issue of regulated emissions from ethanol fumigation (*6, 7*). Little work, however, has focusedonthe health-related properties of these emissions. Particle-related health effects are still not understood entirely, but a widely accepted hypothesis for the many adverse health effects induced by particles is that the particles contain or are able to generate reactive oxygen species (ROS) and, thus, induce oxidative stress at the sites of deposition (*16, 17*). In addition to the particle-induced generation of ROS, several studies have shown that particles may also contain ROS (*18, 19*). As a result, knowledge of the amount of particulate matter (PM) related ROS would assist in assessing the potential toxicological impact of particle emissions from engines that employ ethanol fumigation technology.

To address the lack of data on the emissions of ROS from CI engines, a novel profluorescent nitroxide probe, BPEAnit, was used to detect and quantify the amount of ROS and free radicals generated from neat diesel and ethanol fumigated particle emissions. BPEAnit is a weakly fluorescent compound, but it exhibits strong fluorescence upon radical trapping or redox activity (*20*). Thismakesit a powerful optical sensor for radicals and redox active compounds. The collection of other data involved using a V-TDMA system to explore the volatile properties of particles along with a Dust- Trak to measure PM2.5 emissions.

TABLE 1: **Speed, Load, and Fuel Settings Used for Both Experimental Campaigns**

_____

Campaign number	Speed (rpm)	Load (%)	Fuels used
1	2000	100%	E0, E10.6, E16.3, E22.9
2	1700	100%	E0,, E40
2	1700	50%	E0, E10, E20, E40
2	1700	25%	E0, E20
2	1700	idle	E0, E10

2. Methodology

2.1. Engine, Fuel, and Testing Specifications. Emissions testing was performed on a pre-Euro I, four-cylinder, Ford 2701C engine. Studying pre-Euro I engines (from an Australian perspective) continues to have relevance because of the large percentage of the truck fleet (~40%) that belongsto this emissions class (*21*). Detailed specifications for the test engine are documented in the Supporting Information for this paper. The engine was coupled to a Froude hydraulic dynamometer to provide a

brake load to the engine. The major components of the dual-fuel system fitted to this engine include an electronically controlled ethanol injector, apump and pressure regulator, a heat exchanger for vaporizing ethanol, and a separate fuel tank and fuel lines. A 1 kWheater positioned downstream of the ethanol injector was required to fully vaporize ethanol for higher ethanol substitutions.

Testing was performed with commercially available 10 ppmsulfur diesel. The ethanol used in testing had a moisture content of 0.55% (by mass) and was denatured with 1% unleaded petrol (by volume) in accordance with the fuel supplier's legal requirements. Two experimental campaigns were conducted. The first was conducted at 2000 rpm, full load, and the second was conducted at intermediate speed (1700 rpm) using four different load settings. Table 1 documents the speed, load, and fuel settings used in both experimental campaigns. "EX" denotes that X% of the total fuel energy was provided by ethanol. Consequently, E0 indicates a test that was conducted with neat diesel.

Apart from the different speed settings used, the biggest difference between the two experimental campaigns involved the ability to control ethanol fumigation percentages. Full percentage ethanol substitutions (such as 20%) could not be achieved in the first experimental campaign because of usingan oversized injector that could not provide the required flow rate. This problem was rectified in time for the second experimental campaign.

For each load setting, all tests were conducted at the brake load associated with neat diesel operation. Tests were designed this way so that any change in the emissions was due to the change in fuel and was not due to the different power output of the engine. Data collection did not commence until the exhaust, cooling water, and lubricant temperatures and gaseous emissions had stabilized. To prevent the results from being affected, another test procedure involved flushing the fuel lines of ethanol and leaving the engine to stabilize for approximately half an hour before further tests were conducted.

2.2. Particle Measurement Methodology. A two-stage, unheated dilution system was used to condition exhaust gas before particulate sampling. The first stage of dilution was performed with a dilution tunnel, and the second stage was performed with a Dekati ejector diluter (Dekati, Tampere, Finland). Dilution air was passed through a large HEPA filter to provide particle free air for the primary dilution. Filtered compressed air at 2 bar gauge pressure was fed to the ejector diluter for the second stage of dilution. Particulate mass emissions were measured with a Dust-Trak using a specially designed isokinetic sampling port on the dilution tunnel. CO_2 was used as a tracer gas to calculate dilution ratios.

After the ejector diluter, the aerosol stream was split into three flows for particle size, volatility, and ROS measurements. Figure 1 displays a schematic of the experimental setup used in this study. The methodology for each type of measurement is described below.

Particle number distributions were measured with a scanning mobility particle sizer (SMPS) consisting of a TSI 3071A classifier (EC) and a TSI 3782 condensation particle counter (CPC). Particles within a 10-400nmsize range were measured. For the neat diesel tests, 15 SMPS scans were taken, and at least 5 scans were taken for tests involving ethanol.

2.3. Particle Volatility Methodology. A volatilization tandem differential mobility analyzer (V-TDMA) was used to investigate the volatility of particles (*22, 23*). The system is composed of an electrostatic classifier that preselects particles of a set size followed by a thermodenuder that heats the preselected particles (see Figure 1) to a set temperature. Once particles are heated, the change in particle size is measured with an SMPS. The SMPS consists of an identical classifier to the one that preselects the particles and also consists of a TSI 3010 CPC. The temperature difference between the

saturator and condenser of the CPC was increased to 21 °Cto improve the particle detection efficiency down to 8 nm. The thermodenuder temperature was increased in discrete steps, and the change in the particle diameter was recorded as the volatile components evaporated.

Accumulation mode particles with a diameter of 80 nm were preselected for V-TDMA analysis. Preselecting this particle size was based on themodeof the neat diesel particle size distribution as derived by the SMPS system at full load. Scan times of 90 s were chosen for the SMPS system downstream of the thermodenuder and measured particles within an 8-109.1 nm size range. The thermodenuder was set up to scan temperatures in an approximate range of 30-320 °Cwith temperature increments of 25-30 °Cbetween scans. All testing with the V-TDMA system was performed at intermediate speed. The thermodenuder temperatures were calibrated in the laboratory after testing.

Particle volatilization is presented through the volume fraction remaining (VFR), VFR) (Dv/Dv0)3, where Dv0 is the particle diameter before heating, and Dv is the particle diameter after heating in the thermodenuder to a temperature Td. The dependence of the VFR on thermodenuder temperature provides a volatility signature for particles that enables basic hypotheses regarding the chemical composition and formation mechanisms of particles to be tested. For example, using a V-TDMA system, Sakurai et al. (*24*) demonstrated that diesel nanoparticles had a volatility signature consistent with heavy hydrocarbons (C24-C32) that are prominent constituents of lubricating oil.

In diesel particles, it is common to observe particles of the same size but of significantly different composition and therefore volatility (*24*). Particles such as this are known as external mixtures. As a measure of external mixing, we have quantified the percentage of volatile particles (PVP) according to the following equation:

$$PVP(\%) = 100 \left(\frac{N_{Pre-volatilization} - N_{post-volatilization}}{N_{pre-volatilization}} \right) \tag{1}$$

Where $N_{pre-volatilization}$ is the total particle concentration measured by the V-TDMA before the thermodenuder temperature is increased, and $N_{post-volatilization}$ is the total concentration of the non-volatile peak at the highest temperature applied by the thermodenuder.

2.4. ROS Concentration Measurement: BPEAnit Assay.

Samples were collected by bubbling aerosol for 15-20 min through an impinger containing 20 mL of 4 μM BPEAnit
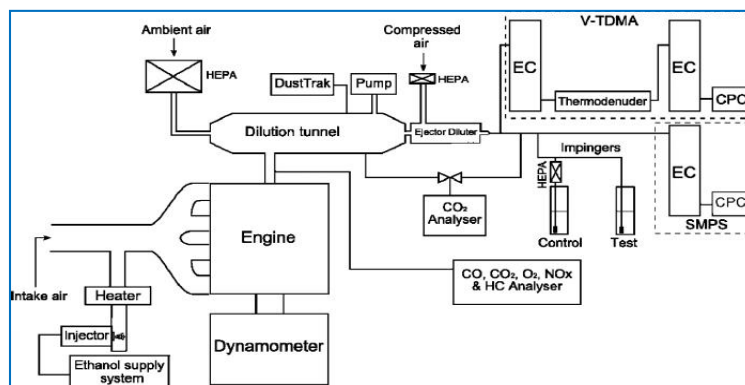

Figure.1: Schematic representation of the experimental configuration used in this study.

solution after which fluorescence was measured. Impingers were placed after the two-stage dilution system. For each fuel type and test mode, fluorescence of both the test and a HEPA filtered control sample was measured.

The new profluorescent nitroxide probe BPEAnit and its methyl adduct (BPEAnit-Me), which was used for the calibration curve, were synthesized in our laboratory. The details of the synthesis are presented in Fairfull-Smith and Bottle (*20*), and details of the evaluation of the probe for applications in particle bound ROS quantification are presented in Miljevic et al. (*25*). The solvent used in all experiments was AR grade dimethyl sulfoxide (DMSO). Impingers used in this study were custom-made and consisted of a Quickfit Dreschel bottle head; they were sintered (porosity grade 1: pore size of 100-160 μm) and were modified to fit a Quickfit 75 mL test tube (Barloworld Scientific, Staffordshire, United Kingdom).

Fluorescence spectra were recorded using a USB2000 fiber-optic spectrometer combined with a cuvette holder and a pulsed xenon lamp (both Ocean Optics, Dunedin, FL) which used a narrow bandpass filter at 430 nm (Edmund Optics, Barrington, NJ). In all of the fluorescence measurements, a 10 mm quartz cuvette (Starna Pty Ltd., Hainault, United Kingdom) was used.

To conduct quantitative chemical analysis on the particles collected by the impingers, it was important to know the collection efficiency of the impinger. This was determined as described in Miljevic et al. (*26*).

The amount of BPEAnit that reacted when exposed to engine exhaustwascalculated from a standard curve obtained by plotting known concentrations of methyl adduct of BPEAnit (BPEAnit-Me; fluorescent) against fluorescence intensity at 485 nm. On the basis of the difference in the fluorescence signal between the test and the control sample, the amount of ROS for each test mode was calculated and normalized to the PM mass calculated from the SMPS data. The portion of particles remaining in the impinger upon bubbling was calculated by multiplying the size distribution by the impinger collection efficiency curve.

3. Results

3.1. Particle Size Distributions. Full-load size distribution data from the SMPS is shown for the neat diesel (E0) and E40
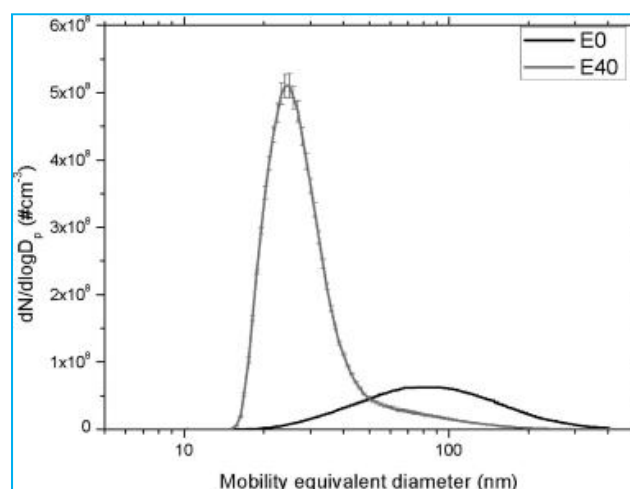

Figure .2: SMPS derived particle number distributions at intermediate speed (1700 rpm), full load, for neat diesel (E0) and 40% ethanol (E40) engine operation. Error bars denote ±one standard error.

test in Figure 2. Full-load size distributions are shown since a clear difference was exhibited for the E0 and E40 tests. Size distributions, at all other loads, for the neat diesel and ethanol tests were quite similar since nucleation occurred in each size distribution.

The mode for the diesel size distribution was about 90 nm, which was in very good agreement with that expected for diesel particulate matter (27). A 40% ethanol substitution (on an energy basis) markedly changed the neat diesel size distribution. The ethanol size distribution had a large peak in the nucleation mode, and it also had a reduced particle mode diameter and reduced accumulation mode particle concentrations.

A correlation between particle size and ethanol substitution is shown in Figure 3 for tests conducted in the first experimental campaign at 2000 rpm, full load. The count median diameter (CMD) of the SMPS-derived particle size distribution was used as a metric for the size of particles. Relative to the neat diesel case (E0), the E22.9 test reduced the CMD by approximately 20% from 81 to 63 nm. It can be seen that the CMD is anticorrelated with the ethanol
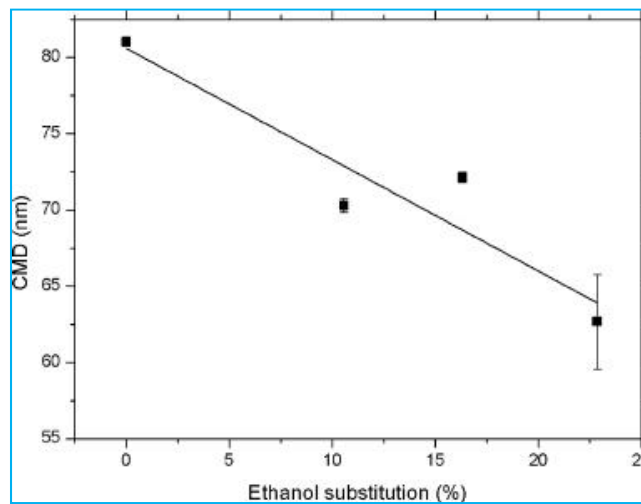

Figure.3: Correlation of particle size (CMD) with the ethanol substitution percentage for tests conducted at 2000 rpm, full load (r) -0.939). Error bars denote ±one standard error.
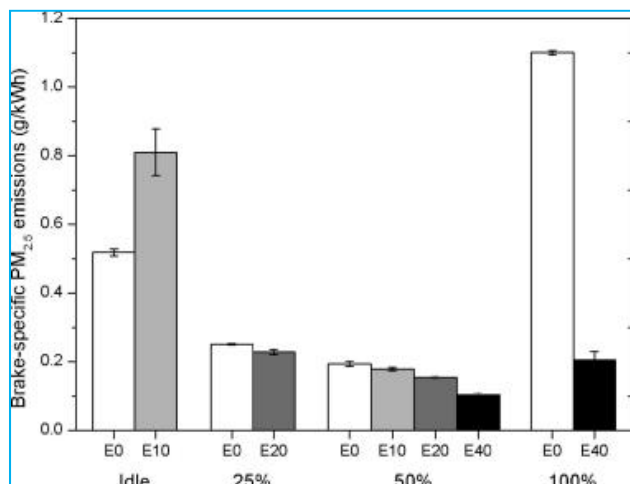

Figure.4: Brake-specific PM2.5 emissions at intermediate speed (1700 rpm) with various load settings and ethanol substitutions. Error bars denote ±one standard error.

substitution percentage (*r*)-0.939), where *r* is the Pearson correlation coefficient.

Brake-specific particulate matter (PM2.5) emissions, for tests conducted at intermediate speed (1700 rpm) and various load settings during the second experimental campaign, are shown in Figure 4. In general, the addition of ethanol significantly reduced PM emissions especially at full-load operation during the E40 test. The results at idle mode were not consistent with the general trend since E10 led to an increase in PM emissions relative to E0. No explanation can be provided for this result. Full-load PM reductions from ethanol were significantly greater than those observed at half or quarter load.

3.2. Particle Volatility. The volume fraction remaining (VFR) curves are displayed in Figure 5a and 5b. It can be observed that for neat diesel at full load (Figure 5a), heating the particles results in a very small reduction in particle volume, while for the E40 test at the same load, there was a significant reduction in particle volume. For loads other than full load, heating of particles introduces a second, far more volatile peak in the size distributions. This more volatile peak separates from the initial distribution of particles preselected for V-TDMA analysis and, consequently, has to be analyzed separately from the less volatile peak for volatilization information (see Figure 5b). Further, significant volatilization occurred between 50 and 100 °C suggesting the presence of fuel or lubricating oil derived organic material
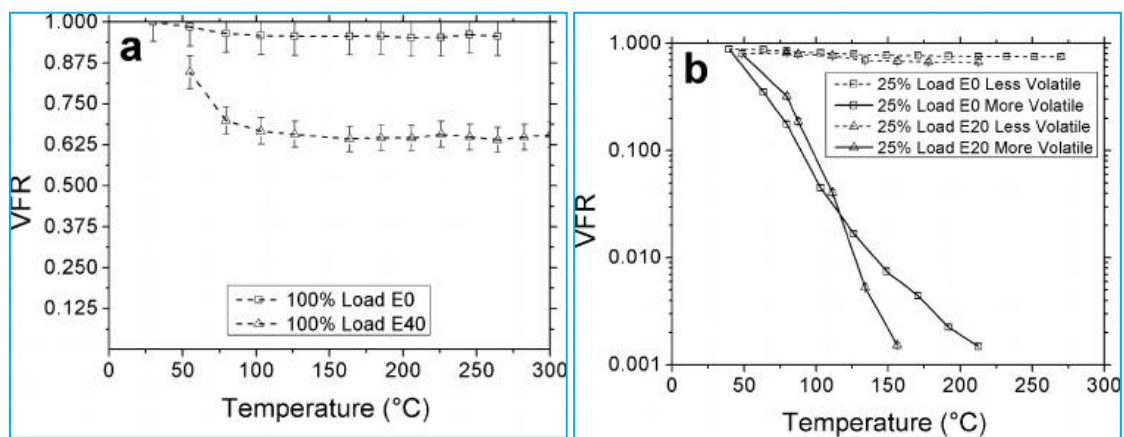

Figure.5: Volume fraction remaining (VFR) versus thermodenuder temperature at intermediate speed (1700 rpm). (a) 100% load E0 and E40. (b) 25% load E0 and E20. Note well the linear scale on the ordinate for **a** and the logarithmic scale on the ordinate for **b**. Error bars are calculated using the uncertainties in the diameter measurement.

(*23, 24*). Size distribution information for the V-TDMA scans can be found in the Supporting Information of this paper.

The volatility results require external and internal mixtures to be defined. An external mixture in automotive exhaust entails carbon and other aerosol particles (such as volatile droplets) existing as distinct, or separate, particles. Alternatively, internally mixed particles have the various components incorporated together and could consist of a carbon core coated with other aerosol particles (*28*). The level of external mixture can be presented through the percentage of volatile particles (PVP). Figure 6 presents the PVP as a function of ethanol substitution for three load conditions, namely, idle, 25%, and 50% load. The PVP at full load is not shown as the particles were not externally mixed and, consequently, the PVP was zero. For all three loads, an increase in the percentage of volatile particles was observed with ethanol. For the half-load case, where several ethanol substitutions were measured,

a clear increasing trend in PVP can be observed with higher ethanol substitutions. The volume fraction of organic material coating the non-volatile particles increased with increasing ethanol substitutions at all loads with results appearing in the Supporting Information of this paper (see Figure S2).

3.3. ROS Concentration Results. Figure 7 shows fluorescence emissions for the BPEAnit solution when exposed to diesel exhaust, and also for the HEPA-filtered control samples, at intermediate speed (1700 rpm) and full load for the neat diesel (E0) and 40% ethanol (E40) tests. There was an increase in the fluorescence signal for BPEAnit when exposed to the engine's exhaust with the fluorescence signal
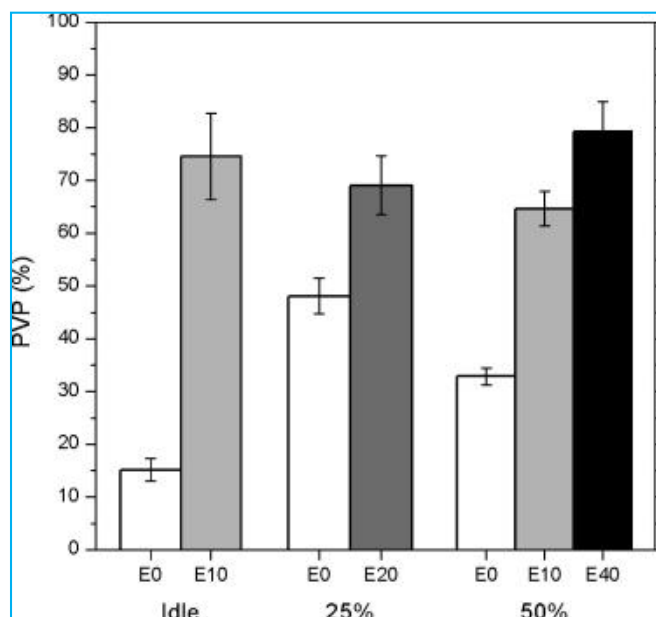

Figure.6: Percentage of volatile particles at intermediate speed (1700 rpm) and 50%, 25% load and idle mode for various ethanol substitutions. Error bars have been calculated using the statistical uncertainty in the particle counts (σ) 1/_n).
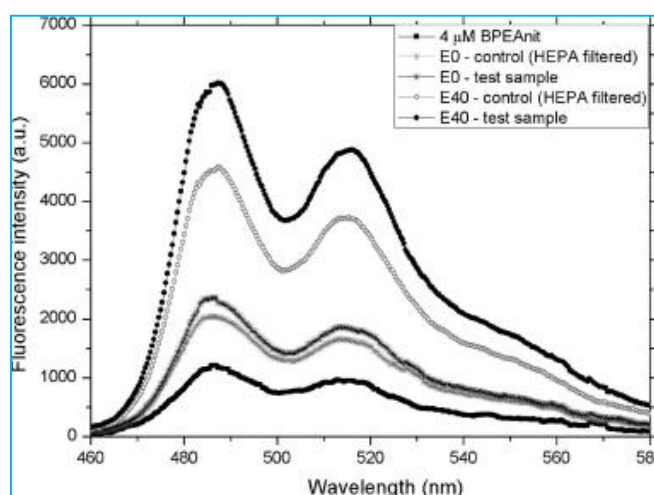

Figure .7: Fluorescence spectra of BPEAnit control (HEPA filtered) and test samples for neat diesel (E0) and 40% ethanol (E40) at intermediate speed (1700 rpm) and full load.

for E40 being significantly higher than for E0. An increase in fluorescence for the HEPA-filtered control samples (gray curves in Figure 7) is due to gaseous reactive species, whereas the fluorescence of test samples (black curves in Figure 7) represents the response due to aerosol being bubbled through the impinger. The difference between the black and the gray curves is, therefore, the fluorescence induced by particles. A small increase in fluorescence was observed for PM emissions from neat diesel testing. On the contrary, PM emissions from the E40 test led to a 4.5-fold increase in fluorescence relative to the neat diesel case.

Normalization of the amount of BPEAnit being converted to fluorescent product with respect to thePMmass represents a measure of ROS concentration. Figure 8 displays ROS concentrations calculated for PM emissions at intermediate speed with various load settings and ethanol substitutions. ROS concentrations for neat diesel emissions at 0 (idle), 25,50, and 100% load show a significant increase with decreasing engine load. ROS concentrations for 10, 20, and 40% ethanol tend to exhibit the same increasing trend as the load is decreased similar to the neat diesel emissions. At a particular load setting, the ROS concentrations for the E10 and E20 tests, relative to E0, do not differ by any more than 20%. At
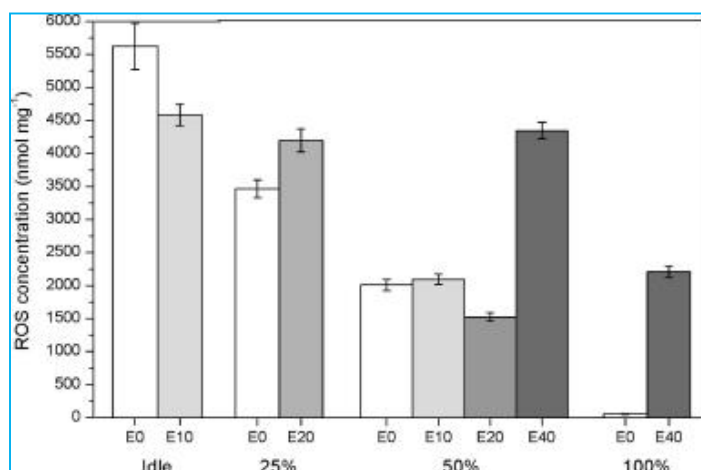

Figure.8: ROS concentrations at intermediate speed (1700 rpm) with various load settings and ethanol substitutions. Error bars denote ± one standard error.

4. Discussion

Several recent papers have addressed the issue of particle number distributions emanating from CI engines using the ethanol blending approach (*11, 13–15*). Although measurements were taken at different speeds, and at different loads and ethanol blend percentages, a common feature of the work of Di et al. (*11, 13*) and Lapuerta et al. (*15*) is that ethanol reduces the peak particle concentration and shifts the CMD of the size distribution to a smaller particle diameter. As a result, ethanol blending technology produces a higher percentage of particles that reside in the ultrafine (<100 nm) size range, but the overall number concentration with ethanol blends is lower relative to the neat diesel case. Using fumigation technology, the result presented in this study (see Figure 2) is different. The reduction in particle concentration in the accumulation mode (>50nm) is still evident, but the concentration in the nucleation mode (<50 nm) is higher by a factor of approximately 8.

The mechanism responsible for nucleation in this case appears to be consistent with a theory developed by Kittelson et al. (*29*). The accumulation mode is very effective at absorbing organic material because of the large surface area available. With the high ethanol substitutions achieved with

fumigation, the accumulation mode surface area is reduced to a level such that organic material has very little particle surface area upon which to condense. Thus, instead of the accumulation mode acting as a "sponge" absorbing organic material and hence reducing its vapor pressure, the organic material resides in the vapor phase with an increased vapour concentration. Under conditions where the vapor pressure of a nucleating species is high and exhaust gas dilution cools the organic material thereby decreasing its saturation vapour pressure, the saturation ratio of organic material is significantly increased and nucleation can occur instead (29). In this case, nucleation occurred solely because of the change in fuel and was not related to some artifact of the dilution process, such as having different dilution ratios or tunnel temperatures during each test. This study provides the first experimental evidence that high ethanol substitutions are capable of inducing nucleation in particle size distributions in addition to decreasing the concentration of particles in the accumulation mode.

Results from the V-TDMA analysis suggest the presence of an organic substance, either derived from fuel or lubricating oil, which coats particles and potentially leaves a sufficient concentration in the vapor phase for nucleation to occur. The amount of volatile material available for nucleation is proportional to the percentage of volatile particles (PVP) and increases with ethanol substitution (see Figure 6). Ethanol fumigation increased the volatility of particulates, either through coating particles with volatile, organic material or through making organic material available for nucleation to occur, producing an external mixture of purely volatile and partially volatile particles.

Ethanol fumigation increased the particle-related ROS concentration, especially at full-load operation, although the ROS concentration was reduced at idle mode operation with E10. The lowest ROS concentration occurred with the full load E0 test, which was the only size distribution measured which did not exhibit a nucleation mode. For all the other tests (involving a nucleation mode), at least a 30-fold increase in ROS emissions occurred relative to the E40 full load test. Therefore, significantly higher ROS concentrations are associated with the formation of nucleation mode particles. An explanation for the mechanism governing the formation of ROS because of ethanol fumigation and its relationship to the formation of a nucleation mode is not possible with the data collected in this study; therefore, further investigation is recommended. The significant increase in potential particle toxicity with ethanol fumigation may provide a substantial barrier for the uptake of fumigation technology using ethanol as a supplementary fuel. Other supplementary fuels should be investigated with fumigation technology to explore the potential toxicological impacts.

The reduction in particle size was also strongly anticorrelated with the percentage of ethanol fumigated (see Figure 3). A possible mechanism for this observation is the oxidation of particulate matter by OH radicals. It has been suggested that OH radicals are much more effective at oxidizing the soot surface than other oxidants such as O_2 (30), which are decreased by ethanol fumigation (see calculation in the Supporting Information) since the intake air is being replaced by fumigated mixture. At temperatures relevant for combustion (1200-2200 K), DalyandNag(31)showedthrough kinetic modeling that the peak concentration of OH radicals during combustion was approximately doubled for a 10% ethanol blend. The concentration of OH radicals tends to peak at the onset of soot depletion (32); therefore, ethanol combustion potentially involves more available oxidant to attack the particle surface and hence to reduce its size. An increase in OH radicals with increasing ethanol fumigation percentages is also confirmed by an AVL Boost simulation conducted as part of this study. The Boost program solves the one dimensional Euler equations for in-viscid, compressible flow and is coupled to a zero-dimensional combustion model. A detailed chemistry module is available in the program for performing emissions simulations (33). Results for this simulation appear in the Supporting Information

A modeling study conducted by Benvenutti et al. (*34*) demonstrated that the methyl radical (CH3) is an important precursor for the formation of excited species such as OH radicals. That fact that the nitroxide probe traps radicals and that, in general, radical concentrations were greater with ethanol fumigation suggests that ethanol combustion provides a pathway capable of significantCH3 and, subsequently, OH radical production. This could also be one of the reasons for a significant increase in the ROS concentration observed with ethanol substitution.

A detailed characterization of particle emission properties has been undertaken for a pre-Euro I engine without after treatment. Newer engine technologies, with after-treatment devices, should be investigated to ascertain if the same qualitative trends are evident.

Acknowledgments

Supporting Information Available

One table and four figures that augment the results presented in the manuscript. This information is available free of charge via the Internet at http://pubs.acs.org/.

Literature Cited

(1) Ahlvik, P. Alternative diesel fuels. In *Dieselnet Technology Guide, Ecopoint Inc*; 2007; http://www.dieselnet.com/tech/fuel_alt. html (accessed May 25, 2009).

(2) Balat, M.; Balat, H.; Oz, C. Progress in bioethanol processing. *Prog. Energy Combust. Sci.* **2008**, *34* (5), 551–573.

(3) Demirbas, A. Progress and recent trends in biofuels. *Prog. Energy Combust. Sci.* **2007**, *33* (1), 1–18.

(4) He, B. Q.; Shuai, S. J.; Wang, J. X.; He, H. The effect of ethanol blended diesel fuels on emissions from a diesel engine. *Atmos. Environ.* **2003**, *37* (35), 4965–4971.

(5) Nord, K.; Haupt, D.; Ahlvik, P.; Egeback, K. Particulate emissions from an ethanol fueled heavy-duty diesel engine equipped with EGR, catalyst and DPF. *SAE Tech. Pap. Ser.* **2004**,*2004-01-1987*.

(6) Abu-Qudais, M.; Haddad, O.; Qudaisat, M. The effect of alcohol fumigation on diesel engine performance and emissions. *Energy Convers. Manage.* **2000**, *41* (4), 389–399.

(7) Ecklund, E. E.; Bechtold, R. L.; Timbario, T. J.; McCallum, P. W. State-of-the-art report on the use of alcohols in diesel engines. *SAE Tech. Pap. Ser.* **1984**, *840118*.

(8) Cheng, C. H.; Cheung, C. S.; Chan, T. L.; Lee, S. C.; Yao, C. D. Experimental investigation on the performance, gaseous and particulate emissions of a methanol fumigated diesel engine. *Sci. Total Environ.* **2008**, *389* (1), 115–124.

(9) Zhang, Z. H.; Cheung, C. S.; Chan, T. L.; Yao, C. D. Emission reduction from diesel engine using fumigation methanol and diesel oxidation catalyst. *Sci. Total Environ.* **2009**, *407* (15), 4497–4505.

(10) Wiesenthal, T.; Leduc, G.; Christidis, P.; Schade, B.; Pelkmans, L.; Govaerts, L.; Georgopoulos, P. Biofuel support policies in Europe: Lessons learnt for the long way ahead. *Renewable Sustainable Energy Rev.* **2009**, *13* (4), 789–800.

(11) Di, Y. G.; Cheung, C. S.; Huang, Z. H. Experimental study on particulate emission of a diesel engine fueled with blended ethanol-dodecanol-diesel. *J. Aerosol Sci.* **2009**, *40* (2), 101–112.

(12) Peters, A.; Wichmann, H. E.; Tuch, T.; Heinrich, J.; Heyder, J. Respiratory effects are associated with the number of ultrafine particles. *Am. J. Respir. Crit. Care Med.* **1997**, *155* (4), 1376– 1383.

(13) Di, Y. G.; Cheung, C. S.; Huang, Z. H. Comparison of the Effect of Biodiesel-Diesel and Ethanol-Diesel on the Particulate Emissions of a Direct Injection Diesel Engine. *Aerosol Sci. Technol.* **2009**, *43* (5), 455–465.

(14) Kim, H.; Choi, B. Effect of ethanol-diesel blend fuels on emission and particle size distribution in a common-rail direct injection diesel engine with warm-up catalytic converter. *Renewable Energy* **2008**, *33* (10), 2222–2228.

(15) Lapuerta, M.; Armas, O.; Herreros, J. M. Emissions from a diesel bioethanol blend in an automotive diesel engine. *Fuel* **2008**, *87* (1), 25–31.

(16) Dellinger, B.; Pryor, W. A.; Cueto, R.; Squadrito, G. L.; Hegde, V.; Deutsch, W. A. Role of free radicals in the toxicity of airborne fine particulate matter. *Chem. Res. Toxicol.* **2001**, *14* (10), 1371– 1377.

(17) Li, N.; Sioutas, C.; Cho, A.; Schmitz, D.; Misra, C.; Sempf, J.; Wang, M. Y.; Oberley, T.; Froines, J.; Nel, A. Ultrafine particulate pollutants induce oxidative stress and mitochondrial damage.*Environ. Health Perspect.* **2003**, *111* (4), 455–460.

(18) Hung, H. F.; Wang, C. S. Experimental determination of reactive oxygen species in Taipei aerosols. *J. Aerosol Sci.* **2001**, *32* (10), 1201–1211.

(19) Venkatachari, P.; Hopke, P. K.; Brune, W. H.; Ren, X. R.; Lesher, R.; Mao, J. Q.; Mitchel,M.Characterization of wintertime reactive oxygen species concentrations in Flushing, New York. *Aerosol Sci. Technol.* **2007**, *41* (2), 97–111.

(20) Fairfull-Smith, K. E.; Bottle, S. E. The Synthesis and Physical Properties of Novel Polyaromatic Profluorescent Isoindoline Nitroxide Probes. *Eur. J. Org. Chem.* **2008**, (32), 5391–5400.

(21) Australian Bureau of Statistics: Motor vehicle census. http://www.ausstats.abs.gov.au/Ausstats/subscriber.nsf/0/ 122DE6BC656964E5CA25753D001199F9/$File/93090_31%20mar% 202008.pdf (Accessed December 10, 2008).

(22) Johnson, G. R.; Ristovski, Z.; Morawska, L. Method for measuring the hygroscopic behaviour of lower volatility fractions in an internally mixed aerosol. *J. Aerosol Sci.* **2004**, *35* (4), 443–455.

(23) Meyer, N. K.; Ristovski, Z. D. Ternary nucleation as a mechanism for the production of diesel nanoparticles: experimental analysis of the volatile and hygroscopic properties of diesel exhaust using

the volatilization and humifidication tandem differential mobility analyzer. *Environ. Sci. Technol.* **2007**, *41* (21), 7309–7314.

(24) Sakurai, H.; Tobias, H. J.; Park, K.; Zarling, D.; Docherty, K. S.; Kittelson, D. B.; McMurry, P. H.; Ziemann, P. J. On-line measurements of diesel nanoparticle composition and volatility. *Atmos. Environ.* **2003**, *37* (9-10), 1199–1210.

(25) Miljevic, B.; Fairfull-Smith, K. E.; Bottle, S. E.; Ristovski, Z. D. The application of profluorescent nitroxides to detect reactive oxygen species derived from combustion generated particulate matter: Cigarette smoke - a case study. *Atmos. Environ.* **2009**,

(26) Miljevic, B.; Modini, R. L.; Bottle, S. E.; Ristovski, Z. D. On the efficiency of impingers with fritted nozzle tip for collection of ultrafine particles. *Atmos. Environ.* **2009**, *43* (6), 1372-1376.

(27) Harris, S. J.; Maricq, M. M. Signature size distributions for diesel and gasoline engine exhaust particulate matter. *J. Aerosol Sci.* **2001**, *32* (6), 749–764.

(28) Jacobson, M. Z. Strong radiative heating due to the mixing state of black carbon in atmospheric aerosols. *Nature* **2001**, *409* (6821), 695–697.

(29) Kittelson, D.; Watts, W.; Johnson, J. *Diesel aerosol sampling methodology CRC E-43, Final Report*; University of Minnesota: Minneapolis, MN, 2002; pp 1-181.

(30) Xu, F.; El-Leathy, A. M.; Kim, C. H.; Faeth, G. M. Soot surface oxidation in hydrocarbon/air diffusion flames at atmospheric pressure. *Combust. Flame* **2003**, *132* (1-2), 43–57.

(31) Daly, D. T.; Nag, P. Combustion modeling of soot reduction in Diesel and Alternate Fuels using Chemkin. *SAE Tech. Pap. Ser.* **2001**, *2001-01-1239*.

(32) Hasse, C.; Bikas, G.; Peters, N. Modeling DI-diesel combustion using the eulerian particle flamelet model (EPFM). *SAE Tech. Pap. Ser.* **2000**, *2000-01-2934*.

(33) AVL LIST GmbH. *AVL Boost, Version 5.1, Users Guide*; Graz, Austria, 2008.

(34) Benvenutti, L. H.; Marques, C. S. T.; Bertran, C. A. Chemiluminescent emission data for kinetic modeling of ethanol combustion. *Combust. Sci. Technol.* **2005**, *177* (1), 1–26.